RESEARCH ARTICLE

Scaling of inertial delays in terrestrial mammals

Sayed Naseel Mohamed Thangal[ID]**, J. Maxwell Donelan** *

Department of Biomedical Physiology and Kinesiology, Simon Fraser University, Burnaby, BC, Canada

* mdonelan@sfu.ca

Abstract

As part of its response to a perturbation, an animal often needs to reposition its body. Inertia acts to oppose the corrective motion, delaying the completion of the movement—we refer to this elapsed time as inertial delay. As animal size increases, muscle moment arms also increase, but muscles are proportionally weaker, and limb inertia is proportionally larger. Consequently, the scaling of inertial delays is complex. Our intent is to determine how quickly different sized animals can produce corrective movements when their muscles act at their force capacity, relative to the time within which those movements need to be performed. Here, we quantify inertial delay using two biomechanical models representing common scenarios in animal locomotion: a distributed mass pendulum approximating swing limb repositioning (swing task), and an inverted pendulum approximating whole body posture recovery (posture task). We parameterized the anatomical, muscular, and inertial properties of these models using literature scaling relationships, then determined inertial delay for each task across a large range of movement magnitudes and the full range of terrestrial mammal sizes. We found that inertial delays scaled with an average of $M^{0.28}$ in the swing task and $M^{0.35}$ in the posture task across movement magnitudes—larger animals require more absolute time to perform the same movement as small animals. The time available to complete a movement also increases with animal size, but less steeply. Consequently, inertial delays comprise a greater fraction of swing duration and other characteristic movement times in larger animals. We also compared inertial delays to the other component delays within the stimulus-response pathway. As movement magnitude increased, inertial delays exceeded these sensorimotor delays, and this occurred for smaller movements in larger animals. Inertial delays appear to be a challenge for motor control, particularly for bigger movements in larger animals.

Introduction

Independent of animal size, a fast response time is important to an animal's survival. A tiny shrew needs to react quickly to escape from a predator, and a massive elephant needs to recover quickly from a loss of balance to prevent a fall. Response time—measured as the total delay between the onset of a perturbation and the completion of the corrective movement that

is in response to the perturbation—is not just important for relatively rare escapes and falls, but also for more common motor control tasks. This is because even small time delays can destabilize feedback control, requiring animals to have compensatory neuromechanical strategies [1–4]. Response time is relevant to the control of movement both in terms of its absolute duration and its duration relative to the available movement time. For example, the absolute duration of the corrective response matters to avoid a snakebite, which can be equally deadly for small and large animals alike. And the relative response time matters to avoid a trip when galloping, where the corrective response may need to occur within a limb's swing duration, which takes longer in larger animals [5–7].

Response time is determined, in part, by neuromuscular physiology [2,8–10]. Consider an animal whose foot catches on a vine—the lengthening of the limb muscles activates the stretch reflex, which resists muscle stretch and helps the animal recover its posture [11,12]. This stretch reflex consists of several component delays. There is a sensing delay to detect the stretch and generate action potentials, a nerve conduction delay to conduct the action potentials through the sensory nerve fibres to the spinal cord, and a synaptic delay to process the signal at the sensorimotor synapse. There is another nerve conduction delay as the action potentials are transmitted down the motor nerve fibres, a neuromuscular junction delay to transmit the action potentials across the neuromuscular junction, an electromechanical delay to conduct the action potentials across the muscle and activate the molecular mechanisms involved in cross bridge formation, and a force generation delay for the muscles to develop forces. We group these six component delays together and refer to their sum as "sensorimotor delay" [2].

After the sensorimotor delays, the corrective response to a perturbation often requires that the animal reposition its body. If muscles could instantaneously generate infinite force, or if the body and its segments were massless, this could be accomplished instantly. But of course, muscles have finite strength and bodies have inertia. Consequently, the animal's inertia impedes the acceleration generated by muscles, further delaying response time. We refer to this last contributor to response time as "inertial delay" and define it as the absolute time between the onset of the corrective movement that is in response to a perturbation and the completion of this corrective movement. A corrective movement is a dynamic process whose duration depends on the movement task and the magnitude of this movement. It depends on the corrective movement task because the time to swing a limb to a new position, for example, may be different from that required to reject a push to the torso to avoid a fall. This is because the two tasks involve different muscles, resulting in different force capacities, and different parts of the body, resulting in different inertial properties. It depends on the magnitude of the required movement because, all else being equal, less time is required to accomplish small adjustments to the body's position and velocity than large adjustments. We approximate these dynamic effects of inertia as fixed time delays by determining the duration required for a movement, while controlling for movement magnitude and movement task.

The scaling of inertial delay depends upon how muscle forces, muscle moment arms, and the body's inertial properties change with body size. When compared to small animals, larger animals have larger muscles and longer moment arms which increase joint torque, but also heavier and longer limbs which increase moment of inertia [13,14]. These properties don't scale precisely with simplified scaling rules such as geometric or dynamic similarity [15,16]. Consequently, it is not clear whether allometric scaling of muscle forces and muscle moment arms offset size-dependent increases in inertial properties, or vice versa. A similar principle is evident in the scaling of skeletal stress, where the disadvantages predicted for larger animals when assuming simplified scaling rules are reduced or eliminated by compensatory size-related changes in other factors, such as posture and moment arms [17–19].

Here we seek to understand how inertial delays scale with animal size in terrestrial quadrupedal mammals. Our intent is to determine how quickly different sized animals can produce corrective movements when their muscles act at their force capacity relative to the time within which those movements need to be performed. Towards this goal, we begin by deriving scaling relationships for the time available to produce a corrective movement, which we term "available movement time". Next, we focus our study on two different tasks designed to represent scenarios commonly encountered during animal locomotion. The swing task represents an animal repositioning its limb to produce a corrective foot placement—modeled as a distributed mass pendulum. The posture task represents an animal recovering its posture after a push forward in the sagittal plane—modeled as a point-mass inverted pendulum. We begin this analysis by deriving analytical expressions for the scaling of inertial delay by linearizing both of these models and parameterizing them using simplified scaling rules. This helps build intuition for the dependence of inertial delay on task, movement magnitude, muscle force, muscle moment arm, and inertial properties. Then to obtain more realistic estimates for the scaling of inertial delays, we parameterize the complete nonlinear models with measured values from literature and simulate them numerically. We then estimate response time as the sum of sensorimotor delays and inertial delays. Finally, we compare this required response time to the available movement time to gauge whether relative response times reach magnitudes where they could detrimentally affect motor control.

Scaling of available movement times

We use characteristic movement times to understand how much time an animal has available to respond to a perturbation and complete the corrective movement. We compare response times to these available movement times to gauge whether the time required to respond may hinder neural control of movement. Here, we analytically quantify the scaling of two characteristic movement times which we have chosen to approximate the time it would take an animal to fall to the ground, and the time an animal's leg is in swing phase when running.

As response time becomes longer relative to fall time, it becomes more difficult for an animal to stop a fall and regain balance. To analytically derive the scaling of fall time, consider an animal of mass M, falling from the height of its leg L to the floor under the force of gravity. Here, we assume that animal morphological features scale with geometric similarity. Two animals are geometrically similar if they have exactly the same shape, even if they are of different sizes [19]. More specifically, it requires that linear features between animals, such as leg length, scale with $M^{1/3}$, surface area features scale with $M^{2/3}$, and masses of body segments scale with M^1 [16]. Under these assumptions, the time t_f required for an animal to fall to the floor is given by:

$$t_f = \sqrt{\frac{2L}{g}} \propto \sqrt{L} \propto M^{1/6} \tag{1}$$

where g is the acceleration due to gravity. We have provided a detailed derivation in section A of S1 File. While it would take longer for an animal to fall like an inverted pendulum, rather than crumple to the ground as described above, the dependence on mass would not change. Similar to falling, if response time exceeds the natural time period of the swinging limb, or some fraction of this period, the animal may have difficulty recovering if the swing is perturbed. We used the natural time period of a pendulum with the properties of an animal limb as a proxy for swing duration [20,21]. Assuming geometric similarity, the natural time period

t_s of a pendulum scales as:

$$t_s = 2\pi\sqrt{\frac{L}{g}} \propto \sqrt{L} \propto M^{1/6} \tag{2}$$

Thus, like time to fall, swing period depends on $M^{1/6}$. Swing duration calculations based on values reported in the literature estimate that it scales with $M^{0.14}$ at trot-gallop transition speeds and with $M^{0.13}$ at maximum sprint speeds [2]. Thus, characteristic movement times scale approximately with $M^{1/6}$ based on both theoretical considerations and empirical measurements. We use these characteristic movement times to normalize the absolute response time.

This relative response time is a measure of how long response time is when compared to the time available to complete the response. It is unlikely that animals have to complete a corrective movement in exactly the duration of the swing phase at sprint speeds. It is possible that they can recover from a perturbation if the corrective movements take longer, and it is also possible that the corrective movements have to be completed in an even shorter period of time. Nevertheless, swing duration seems like a reasonable benchmark to complete a corrective movement to foot placement by the same limb that is perturbed rather than distributing the corrective movement across multiple limbs and multiple phases of the gait cycle. Furthermore, swing duration, fall duration, and pendulum period share a common scaling exponent providing us with some assurance that relative response time will not depend strongly on size as a consequence of our choice of the available movement time used to normalize the absolute response time.

A simple model of inertial delay

3.1 Model

To obtain theoretical estimates for the scaling of inertial delays, we first consider a simple pendulum operating in the horizontal plane without the effect of gravity (Fig 1). These equations of motion are linear, allowing us to analytically derive the scaling of inertial delays. These estimates will support subsequent numerical simulations and provide intuition about how various factors contribute to inertial delays. This system is an angular version of a sliding block model and can be analytically described as a double integrator—a simple and well-studied dynamical system [22,23].

3.2 Scaling of model parameters

Assuming the pendulum scales with geometric similarity, its length would change with $M^{1/3}$, mass with M^1 and moment of inertia (ML^2) with $M^{5/3}$. We consider two scenarios for the scaling of maximum muscle force. In the first scenario, we assume that muscle force maintains dynamic similarity between animals of different sizes by scaling force in direct proportion to animal mass: $F_{musc} \propto M^1$ [15]. In the second scenario, we instead assume muscle force scales with cross-sectional area: $F_{musc} \propto M^{2/3}$ [17]. In this simple pendulum model, the applied muscle torque T_{musc} is the product of the muscle force and a constant muscle moment arm R_{musc}:

$$T_{musc} = F_{musc}R_{musc} \tag{3}$$

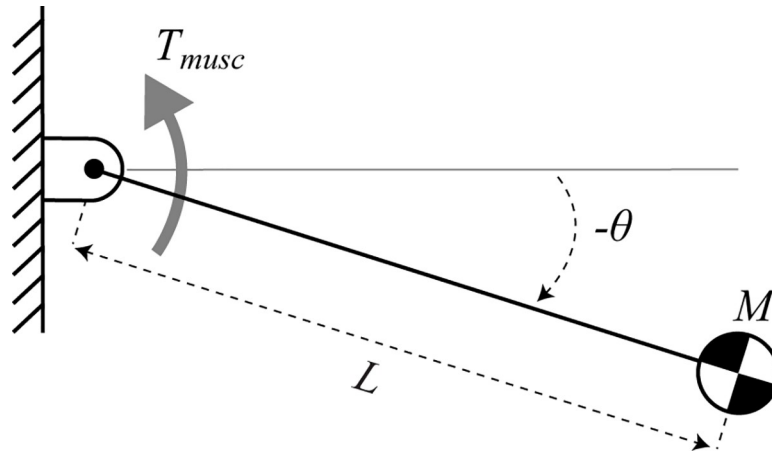We assume that the muscle moment arm scales with geometric similarity ($M^{1/3}$).

Fig 1. Simple model for inertial delay. A pendulum of rod length L and point-mass M rotates about a pin joint actuated by torque T_{musc}. θ is the angle from the horizontal with positive angles in the counter-clockwise direction. This model ignores gravity and assumes the rod is massless.

3.3 Analytical derivation for the swing task

The swing task represents an animal repositioning its swing leg to control foot placement and maintain stability during walking and running [24–28]. For the swing task, the pendulum is required to move through an angular distance $\Delta\theta$ starting from rest, under the control of muscle torque T_{musc}. The inertial delay t_{ID} to reposition the pendulum is given by:

$$t_{ID} = 2\sqrt{\frac{ML^2\Delta\theta}{T_{musc}}} \qquad (4)$$

We have provided a detailed derivation in section B of S1 File. Eq 4 shows that inertial delay is proportional to the square root of both the movement magnitude ($\Delta\theta$) and the moment of inertia of the pendulum (ML^2), and inversely proportional to the square root of the applied torque. Therefore, doubling muscle torque would only result in a 30% reduction in inertial delay. These calculations indicate that while inertial delay does depend on actuator limits, increasing muscle torque may not be an effective option to reduce it.

Next, we consider our two different scenarios for the scaling of muscle force. Beginning with muscle force scaling with dynamic similarity, we determine the scaling of inertial delay by substituting Eq 3 into Eq 4:

$$t_{ID} = 2\sqrt{\frac{ML^2\Delta\theta}{F_{musc}R_{musc}}} = 2\sqrt{\frac{c_1 M^{5/3}\Delta\theta}{c_2 M^{4/3}}} \propto M^{1/6}.\sqrt{\Delta\theta} \qquad (5)$$

where c_1 and c_2 are constants of proportionality. The relative delay t_{rel} scales as:

$$t_{rel} = \frac{t_{ID}}{t_{char}} \propto \frac{M^{1/6}}{M^{1/6}} \propto M^0 \qquad (6)$$

where t_{ID} is the inertial delay. t_{char} is a characteristic movement time representing the available time to produce a corrective movement. t_f and t_s are examples of characteristic movement times (ref. Section 2). Therefore, if muscles produce forces proportional to their mass, inertial delay will scale with the same exponent as characteristic movement times (Eqs 1 and 2), and relative delay would be independent of animal size. To the extent that animals are like this

simple model, large and small animals would be dynamically similar in their response to disturbances and relative delay would not change with animal size. In this scenario, inertial delay would not disproportionately burden larger animals.

Instead, if muscle forces scale with cross-sectional area ($F_{musc} \propto M^{2/3}$), inertial delay scales as:

$$t_{ID} = 2\sqrt{\frac{ML^2\Delta\theta}{F_{musc}R_{musc}}} = 2\sqrt{\frac{c_1 M^{5/3}\Delta\theta}{c_2 M^1}} \propto M^{1/3}.\sqrt{\Delta\theta} \tag{7}$$

$$t_{rel} = \frac{t_{ID}}{t_{char}} \propto \frac{M^{1/3}}{M^{1/6}} \propto M^{1/6} \tag{8}$$

In contrast to dynamic similarity, relative delay will grow with animal size proportional to $M^{1/6}$, when muscle force grows only in proportion to cross-sectional area, penalizing larger animals.

3.4 Analytical derivation for the posture task

The posture task models a standing animal recovering its balance after being perturbed [29–32]. We represent the standing quadruped with a pendulum, which starts from an initial position and has an initial clockwise velocity ($-_A\dot{\theta}_0$) in the sagittal plane due to a perturbation pushing it forward. We define inertial delay as the time required for muscle torque to return the pendulum to rest back at the initial position after recovering from the perturbation. We again use the simple model (Fig 1) and ignore the effects of gravity. The inertial delay t_{ID} to reject the perturbation and return to the vertical position is given by:

$$t_{ID} = (1 + \sqrt{2})\frac{ML^2{}_A\dot{\theta}_0}{T_{musc}} \tag{9}$$

We have provided a detailed derivation in section C of S1 File. Similar to Eq 4 for the swing task, the analytical derivation of Eq 9 gives us insight into how the various factors contribute to inertial delay (t_{ID}) for the posture task. It predicts that the inertial delay during posture recovery after a perturbation is directly proportional to the perturbation size $_A\dot{\theta}_0$ and inversely proportional to the muscle torque T_{musc}.

Since larger animals have heavier bodies, longer limbs and larger muscles, we scaled the size of the perturbation with animal mass to evoke responses with similar relative magnitude. To do this, we express the initial angular velocity of the pendulum, representing the applied perturbation, in terms of linear velocity:

$$_A\dot{\theta}_0 = \frac{v}{L} \tag{10}$$

where v is the linear velocity caused by the initial perturbation and L is the length of the pendulum. We perturbed each model using an initial linear velocity scaled based on a constant dimensionless velocity v_{ND} [33]:

$$v_{ND} = \frac{v}{\sqrt{gL}}, \quad v = v_{ND}\sqrt{gL} \propto M^{1/6} \tag{11}$$

Substituting the values for $_A\dot{\theta}_0$ from Eq 10 and T_{musc} from Eq 3 into Eq 9 and assuming muscle force scales with dynamic similarity ($F_{musc} \propto M^1$) predicts that the inertial delay for the

posture task scales as:

$$t_{ID} = \left(1 + \sqrt{2}\right) \frac{ML^2 v}{F_{musc} R_{musc} L} = \frac{c_1 M^1 M^{2/3} M^{1/6}}{c_2 M^1 M^{1/3} M^{1/3}} \propto M^{1/6}.v_{ND} \tag{12}$$

$$t_{rel} = \frac{t_{ID}}{t_{char}} \propto \frac{M^{1/6}}{M^{1/6}} \propto M^0 \tag{13}$$

If instead muscle force scales with cross-sectional area ($F_{musc} \propto M^{2/3}$), the total time for the posture task would scale as:

$$t_{ID} = \frac{c_1 M^1 M^{2/3} M^{1/6}}{c_2 M^{2/3} M^{1/3} M^{1/3}} \propto M^{1/2}.v_{ND} \tag{14}$$

$$t_{rel} = \frac{t_{ID}}{t_{char}} \propto \frac{M^{1/2}}{M^{1/6}} \propto M^{1/3} \tag{15}$$

Similar to our conclusions from Eq 5 in the swing task, we find that if muscles scaled with dynamic similarity, producing forces proportional to their mass, both inertial delays and characteristic movement times scale with $M^{1/6}$. This results in constant relative delays regardless of animal size. However, if muscles produced forces proportional to their cross-sectional area, inertial delay scales with $M^{1/2}$ in absolute time and $M^{1/3}$ when expressed relative to movement time.

The effect of size on inertial delay depends on the task. The effect of size if muscle forces scaled with cross-sectional area is steeper in the posture task (Eq 14) than what we found in the swing task (Eq 7). An additional difference is the effect of movement magnitude—inertial delay increases in direct proportion to the size of the velocity perturbation in the posture task, and only with the square root of the angular displacement in the swing task. In sections 4 and 5, we use computer simulations of nonlinear biomechanical models, parametrized by actual measurements from literature, to refine our estimates for the scaling of inertial delays.

Swing task

4.1 Model

We modeled the swing task as a distributed mass pendulum actuated by muscle torque (Fig 2). We defined inertial delay for this task as the time required to swing the pendulum from rest at an initial clockwise angle to rest at a final counter-clockwise angle, with identical angles in the clockwise and counter-clockwise direction. Unlike our simple model, we included the effects of gravity, did not assume a point mass, and did not linearize the equation of motion. The motion of the pendulum is described by:

$$\ddot{\theta}(t) = \frac{T_{musc}}{MOI} + \frac{M_{limb} g L_{COM}}{MOI} sin\, \theta(t) \tag{16}$$

where T_{musc} is the muscle torque, L_{COM} is the distance from the pendulum pivot to limb center of mass, M_{limb} is the mass of the limb, and MOI is the moment of inertia of the forelimb about the shoulder joint (Fig 2A). We applied the control torque in a bang-on bang-off profile from $+T_{musc}$ to $-T_{musc}$ to determine a lower bound for inertial delay by ignoring realistic muscle actuation dynamics. In this scenario, inertial delay represents the minimum movement time possible, and is limited only by maximal torque (Fig 2B top panel).
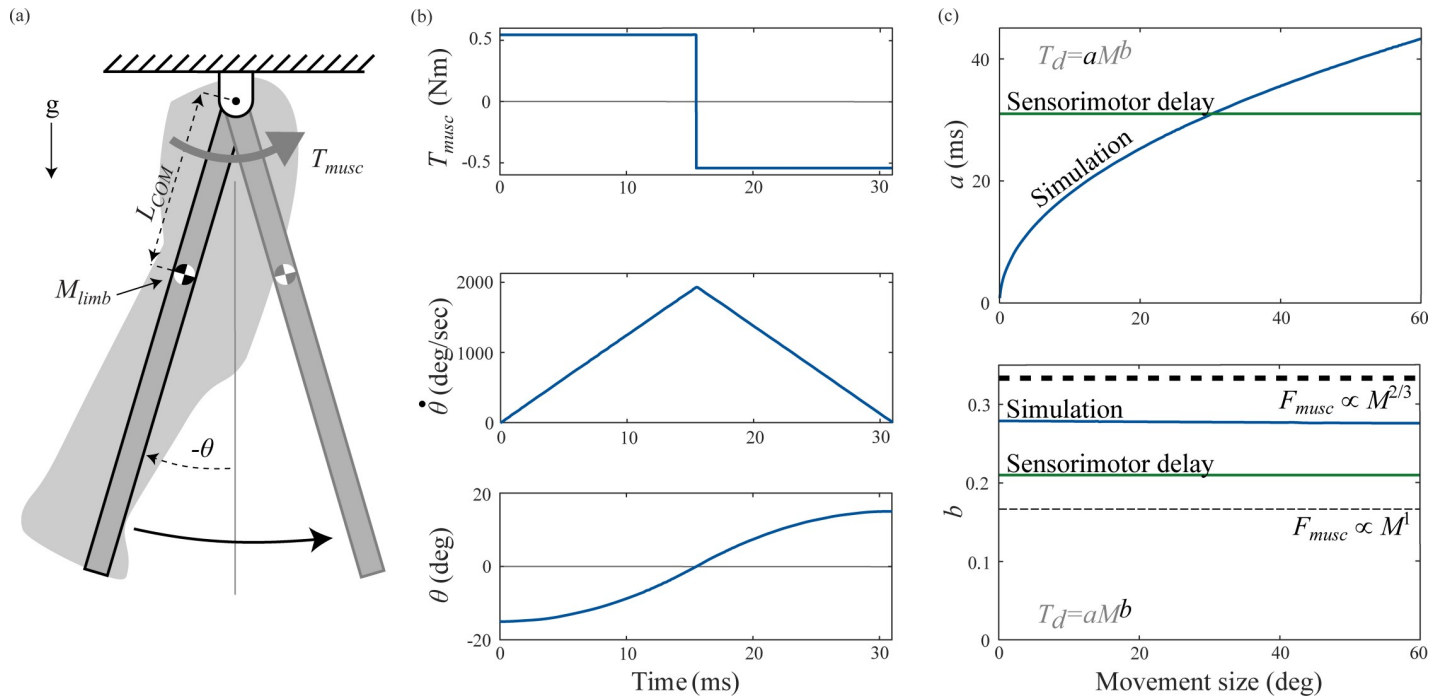
Fig 2. Swing task. The model represents repositioning of the swing leg as part of the response to a trip. (a) We modeled the swing task as a distributed mass pendulum actuated by muscle torque T_{musc}. Our model incorporates the distance from the pendulum pivot to limb center of mass (L_{COM}), mass of the limb (M_{limb}), and moment of inertia of the forelimb about the shoulder joint (MOI). (b) Angle (θ), angular velocity ($\dot{\theta}$), and torque (T_{musc}) profiles in the swing task for a one kg animal for a 30 degree movement, the movement magnitude for which inertial delay equals sensorimotor delay in a one kg animal. (c) Variation in coefficient a and exponent b of the power law for inertial delay from numerical simulations with movement magnitude (dark blue), sensorimotor delay (dark green), and theoretical predictions for the inertial delay exponent based on scaling of muscle force with cross-sectional area $\propto M^{2/3}$ (thick dashed line) and dynamic similarity $\propto M^1$ (thin dashed line).

https://doi.org/10.1371/journal.pone.0217188.g002

4.2 Scaling of model parameters

Table 1 summarizes the scaling relationships we used for our swing task parameters. We used scaling equations for forelimb mass, length, distance from shoulder joint to limb center of mass, and moment of inertia from Kilbourne and Hoffman [14]. We used scaling equations for triceps muscle mass, muscle length, and moment arm from Alexander et al. [13]. We assumed that the triceps is the main muscle flexing the shoulder joint in quadrupeds, because it is a prime mover for this action and because it is the only shoulder muscle for which all the values necessary to compute the scaling of muscle torque are available. Using values for the

Table 1. Swing task scaling parameters and their confidence intervals.

Parameter	Coefficient (a)			Exponent (b)		
	Value	95% CI		Value	95% CI	
Forelimb inertial properties [14]						
Mass (kg)	5.82×10^{-2}	4.61×10^{-2}	7.34×10^{-2}	1.00	0.93	1.08
COM length (m)	5.64×10^{-2}	4.98×10^{-2}	6.38×10^{-2}	0.36	0.32	0.40
MOI (kg m²)	2.52×10^{-4}	1.61×10^{-4}	3.95×10^{-4}	1.75	1.60	1.89
Triceps muscle properties [13]						
Mass (kg)	6.20×10^{-3}	5.54×10^{-3}	6.94×10^{-3}	1.11	1.07	1.15
Muscle length (m)	1.87×10^{-2}	1.72×10^{-2}	2.04×10^{-2}	0.33	0.29	0.37
Moment arm (m)	8.70×10^{-3}	8.13×10^{-3}	9.31×10^{-3}	0.41	0.38	0.44

https://doi.org/10.1371/journal.pone.0217188.t001

entire triceps is a further simplification, as only one of the three heads of the triceps move the shoulder [29]. We assumed that parameters for the shoulder extensor muscles scale in the same way as those for the triceps.

To determine muscle torque for each animal size, we first determined muscle volume by dividing the mass of the muscle by a density of 1060 kg/m³ [34]. We found the muscle cross-sectional area by dividing its volume by the muscle length, assuming that muscles have a consistent cross-sectional area. Multiplying the cross-sectional area by the isometric force generation capacity of mammalian muscle, estimated at 20 N/cm² [35,36], gave muscle force [35,36]. Finally, we calculated muscle torque by multiplying the muscle force and its moment arm (Eq 3).

4.3 Simulation

We performed simulations of the swing task for seven animal masses logarithmically spaced from one gram to ten tons, chosen to span the entire size range of terrestrial mammals [37,38]. For each animal mass, we used the scaling relationships from section 4.2 to determine the size-specific parameters for simulation. At each animal size, we varied the initial clockwise angle from 0.01 to 30 degrees to quantify how movement size affected inertial delay. We numerically simulated the swing task using an explicit Runge-Kutta algorithm implemented with MATLAB's ode45 solver (MATLAB R2017b, The MathWorks, Inc., Natick, MA, USA). We used the solver's event detection to determine when the pendulum reached zero angle and, taking advantage of the symmetric nature of the problem, switched the direction of the applied torque from counterclockwise to clockwise. The simulation continued until the solver's event detection halted the simulation when the pendulum reached zero angular velocity, which occurred when the pendulum reached the same counterclockwise angle as it had started in the clockwise direction. Fig 2B shows an example simulation. Elapsed simulation time was the inertial delay for each animal size and each initial angle. For each initial angle, we then logarithmically transformed the inertial delay values for the various animal sizes and used least squares linear regression to extract the coefficient and exponent for the scaling of inertial delay [39].

We used Monte Carlo simulations to determine 95% confidence intervals for our results by propagating the uncertainty in the input scaling values for limb inertial properties and muscle properties through to our estimates for inertial delay [40,41]. First, we generated probability distributions for each of the limb inertial and muscle properties in Eq 16. For the inertial properties, we fit a linear regression model in MATLAB to the log-transformed raw data from Kilbourne and Hoffman, to generate parameters describing the distribution of the coefficient a and exponent b [14]. For the muscle properties, we did not have access to the raw data so we used the mean and 95% confidence intervals of the scaling parameters to generate t-distributions [13]. We then randomly sampled a single value for each limb inertial and muscle property from their respective probability distribution and used them to simulate our model, generating one scaling coefficient and exponent for inertial delay. We ran 10,000 simulations in this way, obtaining a distribution of coefficients and exponents. Our final 95% confidence intervals are 1.96 times the standard deviations of these distributions. We have provided a detailed description of the Monte Carlo simulations in section D of S1 File.

4.4 Results

Our numerical simulations determined that inertial delay scales with an average of $M^{0.28}$ for the swing task, across movement magnitudes (Fig 2C). This scaling exponent falls between our two analytical predictions, which assume that muscle force scales either with dynamic similarity $M^{1/6}$ (Eq 5) or with muscle cross-sectional area $M^{1/3}$ (Eq 7). The coefficient of inertial delay

in our numerical simulations increased with the square root of movement size (Fig 2C top), as predicted by our analytical analysis (Eq 4). As movement size increased from 1 degree to 60 degrees, the coefficient increased from 5.8 ms (4.0–7.5 ms) to 43 ms (30–57 ms), while the exponent remained fairly steady about 0.28 (0.22–0.34). Here and elsewhere, we report our results as "mean (lower–upper 95% confidence interval)".

We tested the sensitivity of our numerical results to the applied muscle torque. Varying the torque from half to four times its original value only increased the scaling exponent of inertial delay from $M^{0.276}$ to $M^{0.279}$. This indicates that our results for the scaling of inertial delay are robust to possible inaccuracies in our estimates for the torque produced by muscles that flex and extend the shoulder joint. We have provided a short description of these tests in section E of S1 File.

Posture task

5.1 Model

We modeled the posture task as an inverted pendulum that has been pushed in the forward direction resulting in an initial body velocity (Fig 3A). The task goal is to apply the correct muscle forces to reject the perturbation and return the inverted pendulum to rest in an upright posture. We defined inertial delay for this task as the time required to move from a vertical position with an initial velocity perturbation in the clockwise direction to rest at the vertical position, under the control of muscle torque. Unlike our simple model of this task, we included the effects of gravity and did not linearize the equation of motion. The motion of this inverted pendulum model is described by:

$$\ddot{\theta}(t) = \frac{T_{musc}}{ML_{limb}^2} + \frac{MgL_{limb}}{ML_{limb}^2} sin\ \theta(t) \tag{17}$$

where T_{musc} is the muscle torque, L_{limb} is the average length of the forelimb and hindlimb, and M is the total mass of the animal. As in the swing task, we applied the control torque in a bang-on bang-off profile. In this scenario, inertial delay represents the minimum movement time possible, and is limited only by maximal torque.

5.2 Scaling of model parameters

Table 2 summarizes the scaling relationships we used for posture task parameters. We set the length of the inverted pendulum as the average length of the hindlimb and forelimb from Kilbourne and Hoffman, because we wanted the pendulum mass to represent the whole-body center of mass of the animal [14]. In contrast, we set the swing task pendulum length to the length of the forelimb. If we had used the length of the forelimb for the posture task inverted pendulum, our values would increase by 8% or less. We used scaling equations for ankle extensor muscle mass, muscle length, and moment arm from Alexander et al. and computed muscle torque using the steps described in section 4.2 [13]. We assumed that the posture of the animal is controlled by the ankle extensor muscle groups on the four legs by setting T_{musc} to be four times the torque applied by the ankle extensor group.

5.3 Simulation

We performed simulations of the posture task over the same size range as the swing task. For each animal mass, we used the scaling relationships from section 5.2 to determine the size-specific parameters. At each animal size, we scaled the perturbation size based on dimensionless velocity (Eq 11) to evoke a proportional response from each animal size. The inverted
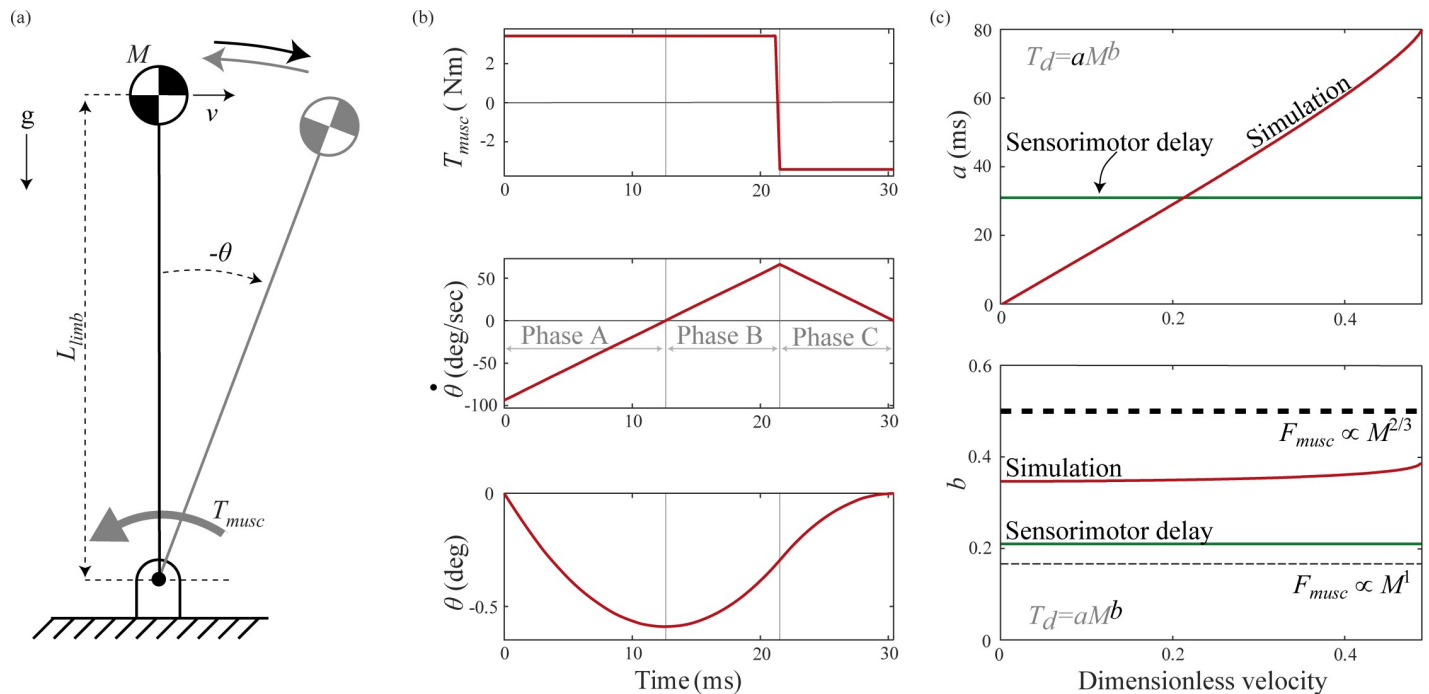
Fig 3. Posture task. The model represents an animal recovering its posture after a perturbation. (a) We use an inverted pendulum with a point-mass body and massless rigid legs, pivoting about a ground-mounted pin joint. Our model considers limb length (L_{limb}), mass of animal (M), and actuating muscle torque (T_{musc}). (b) Angle (θ), angular velocity ($\dot{\theta}$), and torque (T_{musc}) profiles in the posture task for a one kg animal for movement of 0.21 dimensionless velocity, the perturbation size for which inertial delay equals sensorimotor delay in a one kg animal. (c) Variation in coefficient a and exponent b of the power law for inertial delay determined from numerical simulations with perturbation size (red), sensorimotor delay (dark green), and theoretical predictions for the inertial delay exponent based on scaling of muscle force with cross-sectional area $\propto M^{2/3}$ (thick dashed line) and dynamic similarity $\propto M^1$ (thin dashed line).

pendulum can reject the perturbation and return to rest at the vertical position only up to a certain limit—if the initial clockwise velocity is too large, the counter-clockwise torque cannot prevent the inverted pendulum from falling to the ground. The largest perturbation that a 10,000 kg animal could reject and return to vertical was 0.49 dimensionless velocity, so we varied the initial perturbation from 0.01 to 0.49 dimensionless velocity. As with the swing task, we numerically simulated the motion in MATLAB. We used optimization to determine when to switch between the maximum counterclockwise and clockwise torque magnitudes such that the pendulum reached the original upright posture at the same instant the velocity went to zero. For each perturbation magnitude and animal size, we seeded the optimization with an initial guess of the optimal timing and then used the Trust-region dogleg optimization

Table 2. Posture task scaling parameters and their confidence intervals.

Parameter	Coefficient (a)			Exponent (b)		
	Value	95% CI		Value	95% CI	
Limb lengths [14]						
Forelimb length (m)	1.61×10^{-1}	1.42×10^{-1}	1.82×10^{-1}	0.38	0.34	0.42
Hindlimb length (m)	1.63×10^{-1}	1.47×10^{-1}	1.80×10^{-1}	0.36	0.32	0.39
Ankle extensor muscle properties [13]						
Mass (kg)	5.10×10^{-3}	4.40×10^{-3}	5.92×10^{-3}	0.97	0.92	1.02
Muscle length (m)	1.06×10^{-2}	8.98×10^{-3}	1.25×10^{-2}	0.14	0.06	0.22
Moment arm (m)	9.40×10^{-3}	8.79×10^{-3}	1.01×10^{-2}	0.38	0.35	0.41

algorithm (implemented using MATLAB's fsolve function) [42]. It used repeated model simulations to search for the optimal time to switch torque direction. Fig 3 illustrates a representative optimal solution. Elapsed simulation time was the inertial delay for each animal size and perturbation magnitude. Similar to the swing task, we repeated the simulations and optimizations for a range of animal masses and used least squares linear regression to extract the coefficient and exponent for the scaling of inertial delay. We then used Monte Carlo simulations to estimate the 95% confidence intervals. We have provided a detailed description of the Monte Carlo simulations in section D of S1 File.

5.4 Results

Our numerical simulations determined that inertial delay scaled with an average of $M^{0.35}$ for the posture task, across perturbation magnitudes (Fig 3C). The exponent again fell between those of the analytical predictions assuming muscle force scaling based on dynamic similarity ($M^{1/6}$; Eq 12) and on muscle cross-sectional area ($M^{1/2}$; Eq 14). Varying the perturbation size from 0.01 to 0.49 dimensionless velocity caused the coefficient to increase nearly linearly from 1.5 ms (1.1–1.9 ms) to 81 ms (53–102 ms), while the exponent again remained fairly steady about 0.35 (0.24–0.46). This linear dependence on perturbation size was captured by our simple model of this task (Eq 9).

Inertial delays, sensorimotor delays and response time

In both the swing and posture task, inertial delay increases more steeply with animal size than sensorimotor delay. Previous research in our lab has studied sensorimotor delay in terrestrial mammals of varying sizes and found that it scales with $M^{0.21}$ [2]. Here we found that swing and posture task inertial delays scaled with an average of $M^{0.28}$ and $M^{0.35}$ across perturbation magnitudes, respectively. This does not necessitate that inertial delays always exceed sensorimotor delay because inertial delays also depend on the movement magnitude—for very small position changes and velocity perturbations, inertial delays are far shorter than sensorimotor delay at all animal sizes. But as movement magnitudes increase, there reaches a magnitude at which inertial delay first matches, and then exceeds sensorimotor delay. This occurs at smaller movement magnitudes in larger animals (Fig 4). For the swing task, inertial delay exceeded sensorimotor delay when the limb swung through angles greater than $30M^{-0.14}$ degrees, corresponding to 63 degrees in a five gram shrew and only 9 degrees in a five ton elephant. Shrews experience these limb angles only while galloping, but elephants experience them at slower speeds [16]. For the posture task, inertial delay exceeded sensorimotor delay for velocity perturbations greater than $0.21M^{-0.14}$ dimensionless velocity, corresponding to 0.44 in a five gram shrew and only 0.06 in a five ton elephant. For a shrew, this perturbation magnitude is equivalent to its walk-trot transition speed, but for an elephant it is equivalent to a much slower speed [15]. Because day-to-day activities generally involve smaller movements and less extreme perturbations, in most situations sensorimotor delay likely dominates response time for smaller animals while inertial delays dominate for larger animals (Fig 5).

The dependence of both sensorimotor and inertial delays on animal size results in relatively long response times in larger animals. We estimated response time as the sum of sensorimotor delay and inertial delay. If this response time equals or exceeds the available movement duration, an animal cannot complete the task within the available time. Here, we use swing duration at maximum sprint speed, which scales as $148M^{0.13}$ ms, as the available movement time for fast locomotion [2]. We calculate relative response time as the response time normalized by the available time—it scales as $0.42M^{0.08}$. Inertial delay depends on movement magnitude, and here we assumed a 30 degree swing because at this magnitude, inertial delay matches
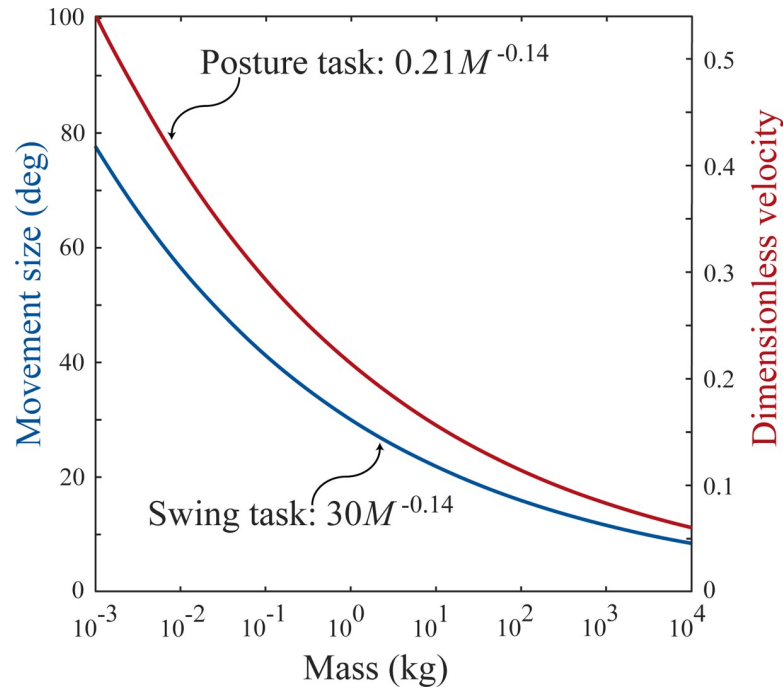
Fig 4. Scaling of movements for which inertial delay equaled sensorimotor delay.

sensorimotor delay in a one kg animal. The fraction of swing duration taken up by sensorimotor delay doubles over seven orders of magnitude of animal mass, while that of inertial delay increases almost six-fold (Fig 5). At maximum running speed, response time requires only about 30% of swing duration for a five gram shrew but about 80% for a five ton elephant. These relatively slower response times in larger animals may hinder their effective control of movement.
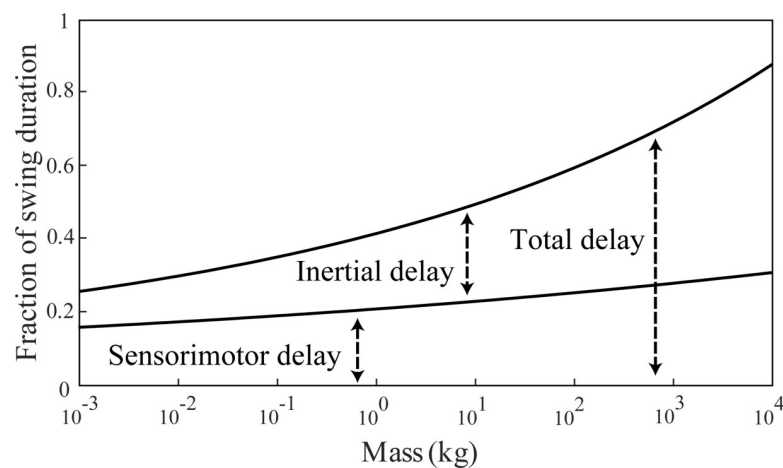
Fig 5. Relative response time. Inertial delay and sensorimotor delay expressed as fractions of swing duration at maximum sprint speed. Inertial delay is shown for a movement of 30 degrees in swing task. At this movement size, inertial delay matches sensorimotor delay in a one kg animal.

Discussion

Here we studied how inertial delays scale with animal size in terrestrial quadrupedal mammals. Inertial delay is the component of response time associated with overcoming inertia to move body segments or reject a perturbation. We quantified it by modeling two scenarios commonly encountered during animal locomotion—a swing task and a posture task. The scaling of inertial delays depended on both the movement task and its magnitude. Over the perturbation magnitudes that we considered, inertial delays scaled with an average of $M^{0.28}$ for the swing task and $M^{0.35}$ for the posture task, which are both steeper than sensorimotor delays at $M^{0.21}$ [2]. We used analytical derivations to show theoretically that if animal muscles could produce forces proportional to an animal's mass, as required for dynamic similarity, inertial delays would scale at the same rate as characteristic movement times and relative delay would be independent of animal size. However, if muscles only produce forces proportional to their cross-sectional area, relative delay would increase with animal size and disproportionately burden larger animals. Our numerical predictions for the scaling exponent fell between these theoretical predictions indicating that muscle forces that scale more steeply than with cross-sectional area, and moment arms that scale more steeply than assumed by geometric similarity, partly, but not completely, overcome the increases in inertia with animal size.

Previous work has suggested that animals may be more acutely challenged by long sensorimotor delays than by inertial delays [14]. Our comparison of these two contributors to response time indicates that this is certainly true in all animals when the movement magnitude is small. But for larger movement magnitudes, including magnitudes encountered during day-to-day movements, inertial delay is greater than sensorimotor delay in larger animals (Fig 4). But sensorimotor delays appear to always be important—response time is never entirely dominated by inertial delay (Fig 5). Whether sensorimotor or inertial delays are more challenging to motor control depends on both the movement magnitude and the animal size.

Our study had several important limitations. First, the lack of literature on scaling of muscle properties constrained the accuracy of our estimates for scaling of muscle torque. To our knowledge, only one study reports the scaling of muscle features necessary for determining torques acting about the shoulder and ankle joints in quadrupedal mammals [13]. Second, due to the lack of data for other muscles, we assumed that the triceps and the ankle extensors are the dominant muscles involved in moving their respective joints and that their antagonistic muscles scale similarly. Thirdly, we assumed that the isometric stress produced by mammalian muscle is constant at 20 N/cm^2 [35], although actual isometric stress values for mammalian muscle vary from 7 to 148 N/cm^2 [43–45]. We tested the sensitivity of our results to muscle torque and found little effect on the exponent of the power law for both tasks (see section E of S1 File). Finally, our models are greatly simplified versions of the rather complex multi-jointed, multi-muscled animal. For example, they do not consider size specific features such as crouch vs columnar posture [17] and high vs low joint damping [46]. A more complete model of different size animals, like might be possible with Open-SIMM or a similar approach, may provide more realistic estimates of inertial delay [47]. However, we don't expect that more complete musculoskeletal models would greatly change the identified scaling exponents which were robust to the major simplifications of the analytical models of Section 3 when compared to our nonlinear simulations in Sections 4 and 5.

Our estimate of response time as the sum of sensorimotor delay and inertial delay makes several simplifications. Firstly, we assumed that muscles can switch between maximal forces instantaneously. However, actual muscles have properties that limit their rate of force production, such as activation-deactivation dynamics and force-velocity properties [36,48–51]. Secondly, we assumed that electromechanical delay, force generation delay and inertial delay are

distinct. However, these component delays are dynamic processes that overlap [2,50]. Thirdly, we have assumed that sensing delay is independent of animal size. This assumption was based on More and Donelan who had previously studied the scaling of sensing delay, but due to scarcity of data, assumed it to be constant at 0.6 ms across animal size [2]. Some sensors, such as muscle spindles, are sensitive to length and length changes [52]. For these sensors, greater inertia may result in longer sensing delays. This is because the same perturbing force will result in slower body accelerations, lower velocities, and smaller length changes of the sensors when inertia is greater. While we have not accounted for this contribution of inertia to sensing delay in our current modeling work, we suspect it is not a major factor—doubling or tripling the nominal sensing delay results in a sensing delay that is still short relative to other contributors. Finally, physiological control rarely works in a purely feedforward fashion without sensory feedback. Feedback control is more resilient to unexpected perturbations and to the inherent noise and delays in biological control systems [53,54]. While superior in these regards, it would only slow the response time that we have estimated here—the optimal feedforward control profile operating at the limits to muscle torque yields a response time that is a lower bound on what is possible with feedback control. We suspect that these limitations make our present estimates of response time conservative, and that a refined model or an experimental approach will find response times that exceed available movement times, particularly in large animals at fast speeds.

Given the importance of a short response time in controlling movement, how do animals cope with their relatively long sensorimotor and inertial delays? We suspect that animals benefit from several factors that mitigate the need for rapid response times. In smaller animals, these include the innate biomechanical properties of the musculoskeletal system to rapidly counteract perturbations. These stabilizing properties arise from the intrinsic properties of muscle [55,56], the increased role of joint damping at small sizes [46], and the geometry of the legs [57]. Biomechanical stabilization is likely less important in larger animals that have a more upright posture, and lower joint damping [46,58,59]. Instead, larger animals may benefit from neural prediction to help ameliorate the effects of long response time [1,2,54,60]. This may only be a useful strategy for comparatively large animals, in which the synaptic delays associated with neural computation are short relative to movement durations [2]. The effects of large inertia on control aren't entirely negative—greater inertia also means that an animal can withstand larger external perturbations before being destabilized [14].

Supporting information

S1 File. Supplementary material. In this document, we have provided detailed derivations for our analytical calculations, described the Monte Carlo simulations used to determine confidence intervals, and elaborated on the methods for determining sensitivity to muscle torque. It contains the following sections:
A. Analytical derivation of fall time
B. Analytical derivation for the swing task
C. Analytical derivation for the posture task
D. Determining confidence intervals
E. Effect of changing muscle torque on inertial delay scaling.
(DOCX)

Acknowledgments

We thank David Remy and James Wakeling for insightful comments and suggestions on the project, and the SFU Locomotion Lab for constructive feedback on the manuscript drafts. We

Author Contributions

Conceptualization: Sayed Naseel Mohamed Thangal, J. Maxwell Donelan.

Data curation: Sayed Naseel Mohamed Thangal.

Formal analysis: Sayed Naseel Mohamed Thangal, J. Maxwell Donelan.

Funding acquisition: J. Maxwell Donelan.

Investigation: Sayed Naseel Mohamed Thangal, J. Maxwell Donelan.

Methodology: Sayed Naseel Mohamed Thangal, J. Maxwell Donelan.

Project administration: J. Maxwell Donelan.

Resources: Sayed Naseel Mohamed Thangal, J. Maxwell Donelan.

Software: Sayed Naseel Mohamed Thangal, J. Maxwell Donelan.

Supervision: J. Maxwell Donelan.

Validation: Sayed Naseel Mohamed Thangal, J. Maxwell Donelan.

Visualization: Sayed Naseel Mohamed Thangal, J. Maxwell Donelan.

Writing – original draft: Sayed Naseel Mohamed Thangal.

Writing – review & editing: Sayed Naseel Mohamed Thangal, J. Maxwell Donelan.

References

1. Milton JG. The delayed and noisy nervous system: Implications for neural control. J Neural Eng. 2011; 8: 065005. https://doi.org/10.1088/1741-2560/8/6/065005 PMID: 22058276

2. More HL, Donelan JM. Scaling of sensorimotor delays in terrestrial mammals. Proc R Soc B Biol Sci. 2018; 285: 20180613.

3. Miall RC, Weir DJ, Wolpert DM, Stein JF. Is the cerebellum a smith predictor? J Mot Behav. 1993; 25: 203–216. https://doi.org/10.1080/00222895.1993.9942050 PMID: 12581990

4. Wolpert DM, Miall RC, Kawato M. Internal models in the cerebellum. Trends Cogn Sci. 1998; 2: 338–347. https://doi.org/10.1016/s1364-6613(98)01221-2 PMID: 21227230

5. Alexander RM. Stability and manoeuvrability of terrestrial vertebrates. Integr Comp Biol. 2002; 42: 158–164. https://doi.org/10.1093/icb/42.1.158 PMID: 21708705

6. Heglund NC, Taylor CR. Speed, stride frequency and energy cost per stride: how do they change with body size and gait? J Exp Biol. 1988; 138: 301–318. PMID: 3193059

7. Heglund NC, Taylor CR, McMahon TA. Scaling Stride Frequency and Gait to Animal Size: Mice to Horses. Science. 1974; 186: 1112–1113. https://doi.org/10.1126/science.186.4169.1112 PMID: 4469699

8. More HL, Hutchinson JR, Collins DF, Weber DJ, Aung SKH, Donelan JM. Scaling of sensorimotor control in terrestrial mammals. Proc R Soc B Biol Sci. 2010; 277: 3563–3568.

9. Burke RE, Levine DN, Tsairis P, Zajac FE. Physiological types and histochemical profiles in motor units of the cat gastrocnemius. J Physiol. 1973; 234: 723–748. https://doi.org/10.1113/jphysiol.1973.sp010369 PMID: 4148752

10. Grillner S. The Role of Muscle Stiffness in Meeting the Changing Postural and Locomotor Requirements for Force Development by the Ankle Extensors. Acta Physiol Scand. 1972; 86: 92–108. https://doi.org/10.1111/j.1748-1716.1972.tb00227.x PMID: 4638321

11. Zehr EP, Stein RB. What functions do reflexes serve during human locomotion? Prog Neurobiol. 1999; 58: 185–205. https://doi.org/10.1016/s0301-0082(98)00081-1 PMID: 10338359

12. Lloyd DPC. Conduction and synaptic transmission of the reflex response to stretch in spinal cats. J Neurophysiol. 1943; 6: 317–326. https://doi.org/10.1152/jn.1943.6.4.317

13. Alexander RM, Jayes AS, Maloiy GMO, Wathuta EM. Allometry of the leg muscles of mammals. J Zool. 1981; 194: 539–552. https://doi.org/10.1111/j.1469-7998.1981.tb04600.x

14. Kilbourne BM, Hoffman LC. Scale effects between body size and limb design in quadrupedal mammals. PLoS One. 2013; 8: e78392. https://doi.org/10.1371/journal.pone.0078392 PMID: 24260117

15. Alexander RM, Jayes AS. A dynamic similarity hypothesis for the gait of quadruped mammals. J Zool. 1983; 201: 135–152.

16. McMahon TA. Using body size to understand the structural design of animals: quadrupedal locomotion. J Appl Physiol. 1975; 39: 619–627. https://doi.org/10.1152/jappl.1975.39.4.619 PMID: 1194153

17. Biewener AA. Scaling body support in mammals: limb posture and muscle mechanics. Science. 1989; 245: 45–48. https://doi.org/10.1126/science.2740914 PMID: 2740914

18. Biewener AA. Biomechanics of mammalian terrestrial locomotion. Science. 1990; 250: 1097–1103. https://doi.org/10.1126/science.2251499 PMID: 2251499

19. Alexander RM. Principles of animal locomotion. 1st ed. Princeton, New Jersey: Princeton University Press; 2003.

20. Mochon S, McMahon TA. Ballistic Walking. J Biomech. 1980; 13: 49–57. https://doi.org/10.1016/0021-9290(80)90007-x PMID: 7354094

21. Halliday D, Resnick R, Walker J. Fundamentals of Physics. 9th ed. New York, NY: John Wiley & Sons; 2010.

22. Rao VG, Bernstein DS. Naive control of the double integrator. IEEE Control Syst Mag. 2001; 21: 86–97. https://doi.org/10.1109/37.954521

23. Srinivasan M. Fifteen observations on the structure of energy-minimizing gaits in many simple biped models. J R Soc Interface. 2010; 8: 74–98. https://doi.org/10.1098/rsif.2009.0544 PMID: 20542957

24. Wong JD, Donelan JM. Principles of energetics and stability in human locomotion. In: Goswami A, Vadakkepat P, editors. Humanoid Robotics: A Reference. Dordrecht: Springer; 2017.

25. Kuo AD. Stabilization of Lateral Motion in Passive Dynamic Walking. Int J Rob Res. 1999; 18: 917–930. https://doi.org/10.1177/02783649922066655

26. Mcgeer T. Passive Bipedal Running. Proc R Soc Ser B-Biological Sci. 1990; 240: 107–134.

27. Daley MA, Biewener AA. Running over rough terrain reveals limb control for intrinsic stability. Proc Natl Acad Sci. 2006; 103: 15681–15686. https://doi.org/10.1073/pnas.0601473103 PMID: 17032779

28. Seyfarth A, Geyer H, Herr H. Swing-leg retraction: a simple control model for stable running. J Exp Biol. 2003; 206: 2547–2555. https://doi.org/10.1242/jeb.00463 PMID: 12819262

29. Rushmer DS, Russell CJ, Macpherson J, Phillips JO, Dunbar DC. Automatic postural responses in the cat: responses to headward and tailward translation. Exp brain Res. Springer; 1983; 50: 45–61. https://doi.org/10.1007/BF00238231 PMID: 6641850

30. Winter DA. Human balance and posture control during standing and walking. Gait Posture. 1995; 3: 193–214.

31. Horak FB, Nashner LM. Central programming of postural movements: adaptation to altered support-surface configurations. J Neurophysiol. 1986; 55: 1369–1381. https://doi.org/10.1152/jn.1986.55.6.1369 PMID: 3734861

32. Ting LH, Macpherson JM. Ratio of Shear to Load Ground-Reaction Force May Underlie the Directional Tuning of the Automatic Postural Response to Rotation and Translation. J Neurophysiol. 2004; 92: 808–823. https://doi.org/10.1152/jn.00773.2003 PMID: 15084643

33. Hof AL. Scaling gait data to body size. Gait Posture. 1996; 3: 222–223. https://doi.org/10.1016/0966-6362(95)01057-2

34. Méndez J, Keys A. Density and composition of mammalian muscle. Metab Exp. 1960; 9: 184–188.

35. Rospars J-P, Meyer-Vernet N. Force per cross-sectional area from molecules to muscles: a general property of biological motors. R Soc open Sci. The Royal Society; 2016; 3: 160313. https://doi.org/10.1098/rsos.160313 PMID: 27493785

36. Close RI. Dynamic properties of mammalian skeletal muscles. Physiol Rev. 1972; 52: 129–197. https://doi.org/10.1152/physrev.1972.52.1.129 PMID: 4256989

37. Jürgens KD. Etruscan shrew muscle: the consequences of being small. J Exp Biol. 2002; 205: 2161–2166. PMID: 12110649

38. Larramendi A. Shoulder height, body mass, and shape of proboscideans. Acta Palaeontol Pol. BioOne; 2015; 61: 537–574.

39. LaBarbera M. Analyzing Body Size as a Factor in Ecology and Evolution. Annu Rev Ecol Syst. 1989; 20: 97–117. https://doi.org/10.1146/annurev.es.20.110189.000525

40. Preacher KJ, Selig JP. Advantages of Monte Carlo Confidence Intervals for Indirect Effects. Commun Methods Meas. 2012; 6: 77–98. https://doi.org/10.1080/19312458.2012.679848

41. Buckland ST. Monte Carlo Confidence Intervals. Biometrics. 1984; 40: 811–817. https://doi.org/10.2307/2530926

42. Powell MJD. A FORTRAN subroutine for solving systems of nonlinear algebraic equations. Atomic Energy Research Establishment. Harwell (England); 1968.

43. Rajagopal A, Dembia CL, DeMers MS, Delp DD, Hicks JL, Delp SL. Full body musculoskeletal model for muscle- driven simulation of human gait. IEEE Trans Biomed Eng. 2016; 63: 2068–2079. https://doi.org/10.1109/TBME.2016.2586891 PMID: 27392337

44. Medler S. Comparative trends in shortening velocity and force production in skeletal muscles. Am J Physiol Integr Comp Physiol. 2002; 283: R368–R378. https://doi.org/10.1152/ajpregu.00689.2001 PMID: 12121850

45. Buchanan TS. Evidence that maximum muscle stress is not a constant: differences in specific tension in elbow flexors and extensors. Med Eng Phys. 1995; 17: 529–536. https://doi.org/10.1016/1350-4533(95)00005-8 PMID: 7489126

46. Garcia MS, Kuo AD, Peattie A, Wang P, Full RJ. Damping And Size: Insights And Biological Inspiration. International Symposium on Adaptive Motion of Animals and Machines. 2000.

47. Delp SL, Anderson FC, Arnold AS, Loan P, Habib A, John CT, et al. OpenSim: Open-source software to create and analyze dynamic simulations of movement. IEEE Trans Biomed Eng. 2007; 54: 1940–1950. https://doi.org/10.1109/TBME.2007.901024 PMID: 18018689

48. Zajac FE. Muscle and tendon: properties, models,scaling, and application to biomechanics and motor control. Crit Rev Biomed Engin. 1989; 17: 359–411.

49. Loeb GE, Pratt CA, Chanaud CM, Richmond FJR. Distribution and innervation of short, interdigitated muscle fibers in parallel-fibered muscles of the cat hindlimb. J Morphol. 1987; 191: 1–15. https://doi.org/10.1002/jmor.1051910102 PMID: 3820310

50. Mörl F, Siebert T, Schmitt S, Blickhan R, Günther M. Electro-mechanical delay in hill-type muscle models. J Mech Med Biol. 2012; 12: 1250085. https://doi.org/10.1142/S0219519412500856

51. Rios E, Pizarro G, Stefani E. Charge movement and the nature of signal transduction in skeletal muscle excitation-contraction coupling. Annu Rev Physiol. 1992; 54: 109–133. https://doi.org/10.1146/annurev.ph.54.030192.000545 PMID: 1562172

52. Matthews PB. Muscle spindles and their motor control. Physiol Rev. 1964; 44: 219–288. https://doi.org/10.1152/physrev.1964.44.2.219 PMID: 14152906

53. Todorov E, Jordan MI. Optimal feedback control as a theory of motor coordination. Nat Neurosci. 2002; 5: 1226–1235. https://doi.org/10.1038/nn963 PMID: 12404008

54. Kuo AD. The relative roles of feedforward and feedback in the control of rhythmic movements. Motor Control. 2002; 6: 129–145. https://doi.org/10.1123/mcj.6.2.129 PMID: 12122223

55. Brown I, Loeb G. A reductionist approach to creating and using neuromusculoskeletal models. Biomech neural Control posture Mov. 2000; 148–163. https://doi.org/10.1007/978-1-4612-2104-3_10

56. Gerritsen KG, van den Bogert a J, Hulliger M, Zernicke RF. Intrinsic muscle properties facilitate locomotor control—a computer simulation study. Motor Control. 1998; 2: 206–220. https://doi.org/10.1123/mcj.2.3.206 PMID: 9644290

57. Biewener AA. Scaling body support in mammals: limb posture and muscle mechanics. Science. 1989; 245: 45–48. https://doi.org/10.1126/science.2740914 PMID: 2740914

58. Hooper SL, Guschlbauer C, Blümel M, Rosenbaum P, Gruhn M, Akay T, et al. Neural control of unloaded leg posture and of leg swing in stick insect, cockroach, and mouse differs from that in larger animals. J Neurosci. 2009; 29: 4109–4119. https://doi.org/10.1523/JNEUROSCI.5510-08.2009 PMID: 19339606

59. Hooper SL. Body size and the neural control of movement. Curr Biol. 2012; 22: R318–R322. https://doi.org/10.1016/j.cub.2012.02.048 PMID: 22575473

60. Wolpert DM, Ghahramani Z. Computational principles of movement neuroscience. Nat Neurosci. 2000; 3: 1212–1217. https://doi.org/10.1038/81497 PMID: 11127840